SAND2011-9460C

Wind Turbine Structural Path Stress and Fatigue Reductions Resulting from Use of Active Aerodynamic Load Control

Brian Resor, Dale E. Berg*

Sandia National Laboratories†, Albuquerque, NM, USA, 87111

Zachary Wright, Chris Halse, Ashley R. Crowther

Romax Technology Ltd, Boulder, CO USA 80301

Active aerodynamic load control has been used in simulation to improve fatigue life of wind turbine blades. A side effect of load control is a balancing of the thrust load on the rotor in such a manner that reduces the non-torque loads on the turbine drivetrain components. Reduction of these loads may lead to significant improvements in their lifetime and reliability. This paper demonstrates simulations and results that quantify some of these beneficial effects.

I. Introduction

In the first decade of the 21st century the wind industry grew at rates consistently above 20% a year in terms of global cumulative installed capacity (MW), according to the Global Wind Energy Council[1], as illustrated in Figure 1. In 2009 the growth was 31% despite the global economic crisis. Accompanying this rapidly expanding market and the attendant growth in machine size are significant issues with the reliability in the drive train, electrical systems, pitch systems and yaw systems. Tavner, et al.[2] present reliability statistics for a European database of wind turbine failures and the analysis of the LWK[3] survey of 643 wind turbines. This information is summarized below in Figure 2 and Figure 3. These statistics show the gearbox, main shaft, pitch and yaw systems all have significant failure rates and, in particular, failures in the drivetrain bring the highest downtime.

These reliability issues threaten the sustained growth of the market; the need for improved reliability and robust designs has brought an industry wide effort to address these issues. Evidence of this effort is found in the development of a new IEC standard 61400-4, *'Wind Turbines - Part 4: Design and Specification of Gearboxes'* (replacing ISO 81400-4:2005), the National Renewable Energy Laboratory Gearbox Reliability Collaborative (NREL GRC)[4] and the establishment of the Sandia National Laboratories Database Continuous Reliability Enhancements for Wind (CREW) Database[5].

The wind-induced loads on a large rotating wind turbine blade vary quickly in time and space due to the stochastic nature of the wind and the fact that the sizes of coherent structures in the wind (the gusts) are significantly smaller than the length of the blades. The resulting blade oscillating (or fatigue) loads can be design drivers for the turbine blades and some components of the drive train.

---

* Members of the Technical Staff, Wind Energy Technologies Department, PO Box 5800 MS1124

†Sandia is a multiprogram laboratory operated by Sandia Corporation, a Lockheed Martin Company, for the United States Department of Energy's National Nuclear Security Administration under contract DE-AC04-94AL85000.

According to the DOE "20% Wind Energy by 2030"[6] report, one way to reduce COE "…lies in an active control that senses rotor loads and actively suppresses the loads transferred from the rotor to the rest of the turbine structure. These improvements will allow the rotor to grow larger and capture more energy without changing the balance of the system." In particular, one concept for suppressing the fatigue loads acting on large turbine blades is to implement small, fast response, aerodynamic control devices (with associated sensors and control systems to sense the existing loading and direct appropriate control device action) distributed along each blade to provide feedback load control (often referred to in popular terms as 'smart structures' or 'smart rotor control'). A recent review of this concept, including a discussion of the feasibility of the concept and an inventory of design options for such systems, has been performed by Barlas and van Kuik at Delft University of Technology (TUDelft)[7]. One attractive control device design option is that of utilizing trailing edge flaps or deformable trailing edge geometries; this option is referred to here as Active Aerodynamic Load Control or AALC. This technology is a focus of research at several locations, because of the direct lift control capability of trailing edge devices and recent advances in smart material actuator technology. Researchers at TUDelft[8,9], Risø Danish Technical University National Laboratory for Sustainable Energy (Risø/DTU)[10-16] and Sandia National Laboratories (SNL)[17-21] have been active in this area over the past several years. Researchers at SNL have performed extensive simulations of AALC on several turbine configurations and have analyzed the simulation results to estimate the potential fatigue damage reduction benefits of AALC and the decreases in cost of energy that might result from integrating AALC technology into turbine blades.

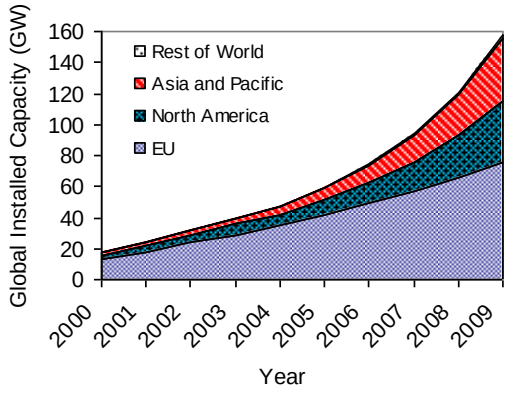

Figure 1 Global installed capacity from 2000-2009[1]

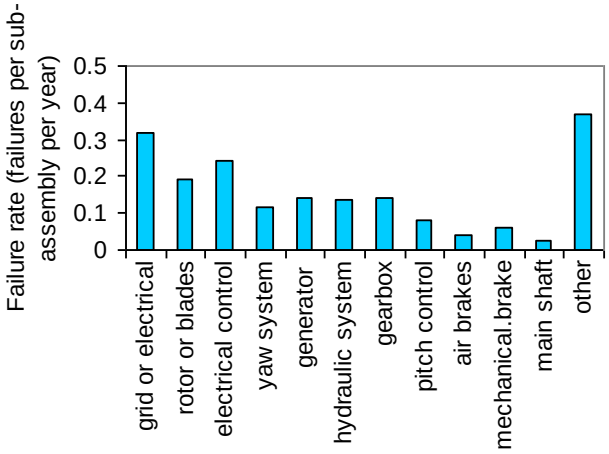

Figure 2 Failure rate of wind turbine components[2].

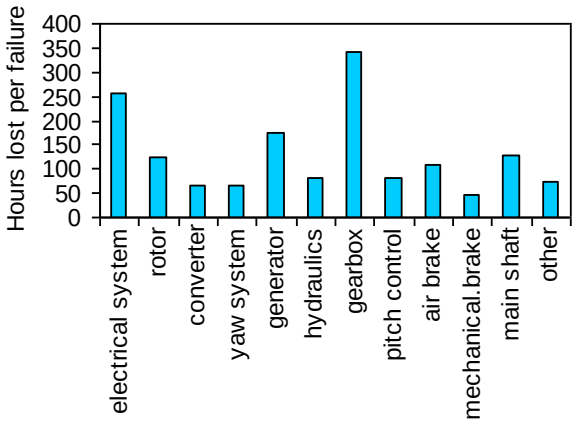

Figure 3 Hours lost per failure for wind turbine components[2].

The focus of nearly all AALC studies to date has been the reduction of blade fatigue loads. However, reducing ultimate and fatigue loads on wind turbine blades may also result in the modification of loads on other turbine components such as rotor hubs, main bearings, gearboxes, main frames, generators and towers, potentially resulting in large reductions in both the initial capital costs and the maintenance costs. These reductions in loads may, in turn, provide a significant decrease in the resulting overall cost of energy. The Berg et al[21] report, a preliminary study performed in 2010, demonstrated that, as a side effect of controlling the fatigue loads on the rotor of a 1.5MW turbine, AALC also leads to reductions in damaging off-axis oscillatory loading, such as side loads and overturning moment, on a typical turbine gearbox. Those reductions could be expected to lead to reduced gearbox bearing fatigue damage and improved lifetimes. That study suggests that the use of AALC may mitigate damage to all drive train components by reducing the off-axis oscillating loads that the main shaft bearings otherwise have to support.

This current work expands on that preliminary work by examining the impact of AALC on several major components in the structural load path between rotor blades and bed plate.

A. Overview of NREL GRC Project

The National Wind Technology Center (NWTC) has been running the Gearbox Reliability Collaborative project (GRC) for the Department of Energy. This important project brings together gearbox engineers, manufacturers, owners, expert consultants, academics and other partners from the wind industry in an effort to collectively improve gearbox reliability, through improved understanding of the causes of poor reliability. The ultimate goal of this project is to decrease the costs associated with operations and maintenance of these major drivetrain components.

A key goal of the GRC was to comprehensively instrument two gearboxes for measurements of tooth root strains, bearing temperatures, bearing raceway strains, gearbox motion, carrier motion, torque, speed and other parameters to allow a more detailed understanding of the internal behavior of the machinery under operation. This has been a successful phase of the project with tests performed at the NWTC 2.5MW dynamometer facility and in the field at the Ponnequin Wind Farm in northern Colorado. An extensive measurement data set has been collected and collated and now serves as an excellent tool for evaluation and improvement of gearbox design and software tools and for understanding the dynamic behavior of gearbox components.

As part of the GRC analysis team, Romax has validated gearbox CAE models against measured planet-to-ring-gear load distributions using RomaxWind software. The correlation is very good, as documented by Wright, et al.[22] and Crowther, et al.[23], confirming that the many parameters and the basic system physics within the gearbox design are accurately modeled with the software tool. These parameters include clearances in planet carrier bearings and planet bearings, gear geometry and microgeometry, whole system structural deflections leading to certain gear and bearing misalignment, weight loading of components, external loading such as wind turbine rotor bending moments and

torque, bearing and gear Hertzian contact stiffness and deflections and the flexibility of bearing raceways and gear blanks.

This research on active aerodynamics controls utilizes this GRC 750 drivetrain model because it is validated. The credibility of the analyses performed here is improved due to the demonstrated model accuracy.

II. Supporting Models and Simulations

B. RomaxWIND Model of the NREL GRC Drivetrain

Figure 4 provides some information on the GRC drivetrain model; Figure 4a provides an internal view of the RomaxWIND model of the gearbox, including shafts, gears, bearings and torque arms while Figure 4b illustrates the drivetrain layout, including the main shaft, the gearbox and the bedplate. The rotor hub and bedplate are represented as flexible elements in the model. Note that the gearbox design and subsequently the CAE models used for the NREL GRC project have been modified to improve some of the design short-comings outlined in Wright, et al.[22]. Previously reported results by Wright, et al.[22] and Crowther, et al.[23] for gear mesh misalignment between the sun/planet gears and planet/ring gears have been improved by changes to the planetary carrier bearings and to the lead slope corrections applied to the gearing. These improvements to the gearbox allow these studies to focus on the influence of AALC, without the influence of poor design features.

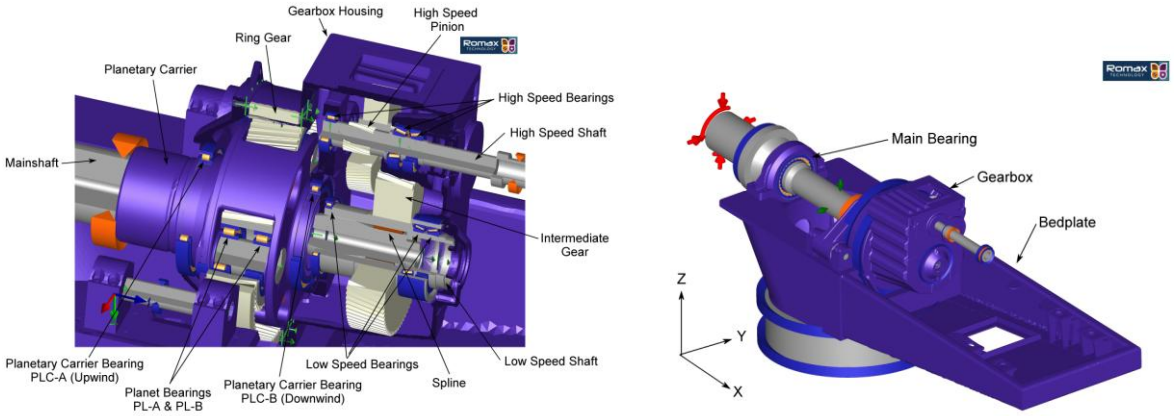

a) Internal View of GRC Gearbox *b) Bedplate Assembly with Coordinates*

Figure 4 RomaxWind model of GRC gearbox showing key features

C. The GRC Turbine

The actual GRC turbine is a fixed-pitch, two-speed, upwind, three-bladed, 750kW machine. The NREL FAST model used for the simulations performed in this work is based on the blade and tower properties documented by Bir and Oyague[24]. In order to represent common utility scale controller behavior, the basic GRC turbine model has been extended for this research by the implementation of a basic Variable-Speed, Variable-Pitch (VSVP) controller.

D. AALC Devices

Simulated AALC devices for this investigation consist of trailing edge flaps (ailerons) placed in the outer 25% of blade span. The flap hinge location is at 80% of blade chord and the flap deflection is limited to +/-10 degrees. The peak rate of flap actuation is limited at approximately 100 degrees per second. Two-dimensional lift and drag

performance of the flapped airfoil sections for various flap deflections were calculated with the XFOIL code[25] and modified with the AirfoilPrep tool[26] to include three-dimensional flow effects of the rotor. Flap lift and drag data is determined during the simulation through use of the *MulTabLoc* variable within FAST, thus the approach basically represents a quasi-steady flapped section response.

E. AALC Controllers

A simple PD controller was developed to activate the trailing edge flaps, in conjunction with the conventional VSVP control, to provide effective cyclic fatigue loads alleviation for this wind turbine. The controller performance index goal maintains maximum power output while minimizing blade-root bending cyclic moments during turbulent wind conditions. No attempt has been made to optimize the span-wise placement or extent of the flaps.

A more detailed description of similar AALC controllers developed for a 1.5MW turbine may be found in Wilson, et al.[17]. Wilson found that both tip deflection and tip-deflection rate controllers were effective in reducing the blade-root flap moment fatigue loading, while having little effect on the rotor speed, the low speed shaft torque, the tower base side-to-side and fore-aft moments, and the tower-top yaw moment responses. The tip deflection controller is used for all the results reported in this paper.

Proportional and derivative gains for the AALC controller are scheduled based on mean incoming wind speed. The gains are chosen to maximize cyclic load reductions while keeping flap actuation rates below approximately 100 degrees per second.

F. Aeroelastic Simulation Process

Turbine component fatigue accumulation calculations require time-series load histories at the turbine locations of interest at a number of mean wind speeds spanning the entire operating range of the turbine. For this work, these load histories are generated with structural dynamic simulations of the GRC turbine performed with the NREL FAST structural dynamics code[27], utilizing the NREL AeroDyn aerodynamic code[28] to compute the aerodynamic forces on the blades. FAST utilizes a modal representation of the turbine to determine its response to applied forces, while AeroDyn utilizes the Blade Element Momentum (BEM) representation of aerodynamic loads, relying on airfoil characteristic lookup tables to determine the load at any angle of attack. A dynamic wake model within Aerodyn incorporates the unsteady effects of the wake on the rotor inflow, and a dynamic stall option incorporates certain unsteady effects due to active flap actuations. The Matlab/Simulink[29] control simulation code is used to model both the standard VSVP controller and the AALC control logic for these simulations. AeroDyn takes advantage of the *MulTabLoc* variable to model the effects of blade trailing edge deflection by selecting appropriate alternate lift and drag curves in response to control input from Simulink. All turbine simulations are driven with 10-minute duration, 3-dimensional turbulent wind fields (IEC Normal Turbulence Model, Type A turbulence[30]) generated with the NREL TurbSim code[31].

TurbSim-generated wind fields are created to yield the appropriate mean wind speed and turbulence levels and statistical behavior, but the actual fields depend upon a random seed number – different seed numbers result in different wind fields. Six 10-minute simulations are run at each mean wind speed (with different random seeds) to develop representative loads distributions. For this effort, simulations are performed at mean wind speeds of 4, 6, 8, 10, 12, 14, 16, 18, 20, 22 and 24m/s.

G. Processing Time-Series Data for Peak Loads

The time series data is processed via search algorithms to construct a peak loads table. For each force and moment, one maximum and one minimum value are found from the combined time histories. The resultant radial transverse force and off-axis moments are calculated and the maximum/minimum values are also found, yielding a peak loads table with 16 columns (8 forces, 8 moments). The peak loads table also records loads in the other directions at the time instant that the peak load occurs. The analyses apply these loads as well as the peak load. Note that the peak loads and results below are described according to the FAST hub non-rotating coordinate system.

III. Results

H. Impact of AALC on the Rotor

Incoming wind speed varies spatially over the diameter of the wind turbine rotor disk. As a result, the center of thrust on the rotor as a whole will vary in time and can produce rather large non-torque moments about the main bearing of the turbine. Active aero load control reacts to the unevenly distributed wind inflow in a manner that tends to balance the thrust load on the rotor, thus encouraging the center of thrust to act closer to the hub and causing lower non-torque loads into the turbine drivetrain. Figure 5 illustrates this point by showing a decrease in the average center of thrust (radial distance from the hub) for the active aero load control simulation.

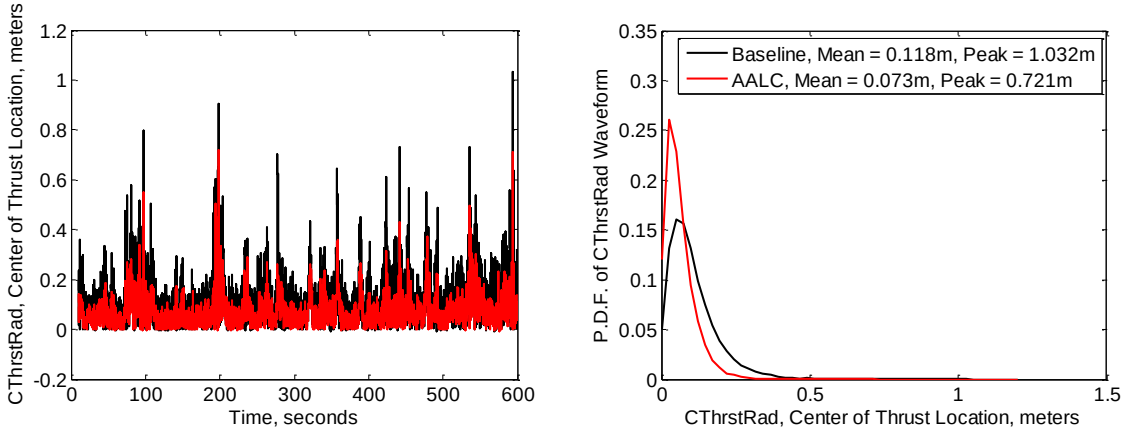

(a) (b)

Figure 5 Location of thrust center for baseline and AALC simulations at 14 m/s average wind speed: (a) time waveforms from FAST simulation and (b) waveform probability distribution function.

I. Impact of AALC on Peak Load Inputs

The peak loads (excluding the resultant minimums) are compared in Figure 6 for the Base case vs. AALC. The reduction in the forces by application of AALC is significant, with the greatest reduction being 12% for the thrust force (F_{xmax}); the reduction in the resultant force (combining F_y and F_z) is 9%. The most significant benefit is the large reduction to the off-axis moments, where the resultant of M_y and M_z is reduced by 70%. This has great influence on the limiting stresses in many structural elements, as will be demonstrated.

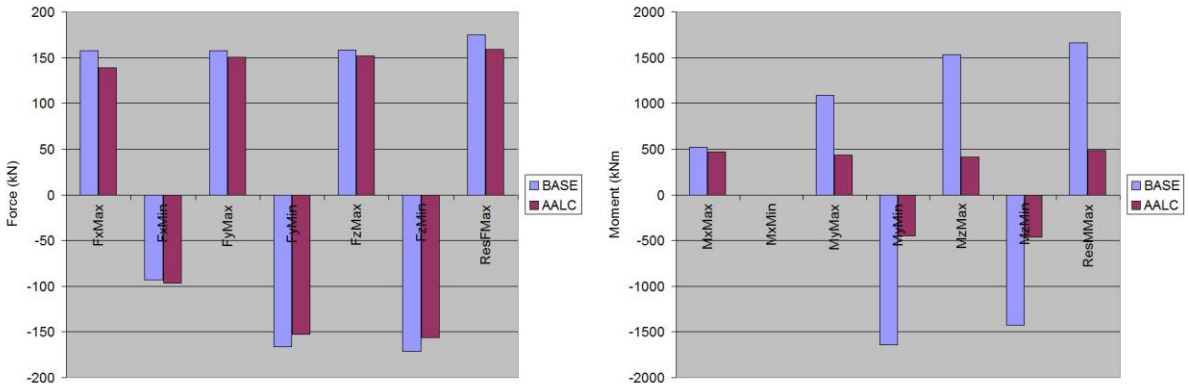

Figure 6 Comparisons for max/min forces and moments (BASE vs. AALC)

J. Impact of AALC on Load Carrying Drivetrain Bearings

The primary non-torque load carrying components in this drivetrain are the main bearing and planet carrier bearings. Within the RomaxWind model a set of analyses is performed for each of the peak load cases. Each analysis requires a non-linear static convergence for the solution, where the input load at the hub includes the peak load and corresponding loads in the other dimensions. The analysis incorporates the elastic deflection of the entire structure while solving the contact problem for gears and bearings. Figure 7 and Figure 8 provide the bearing maximum contact stresses for the peak loads. Adding AALC provides significant improvements. For the main bearing, the maximum contact stresses for the base case fall in the range of 2300-2400MPa for the worst load cases and these are reduced to 1600-1800MPa with AALC. Both planet carrier bearings see a benefit; notably the upwind bearing experiences stress reductions in the order of 50% for the peak moment load cases. The highest stress case (the limiting case) for the upwind carrier bearing is reduced from 2693MPa to 1250MPa.

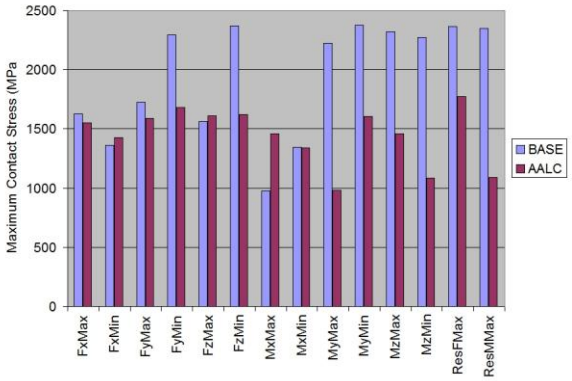

Figure 7 Main bearing contact stress results (BASE vs. AALC)

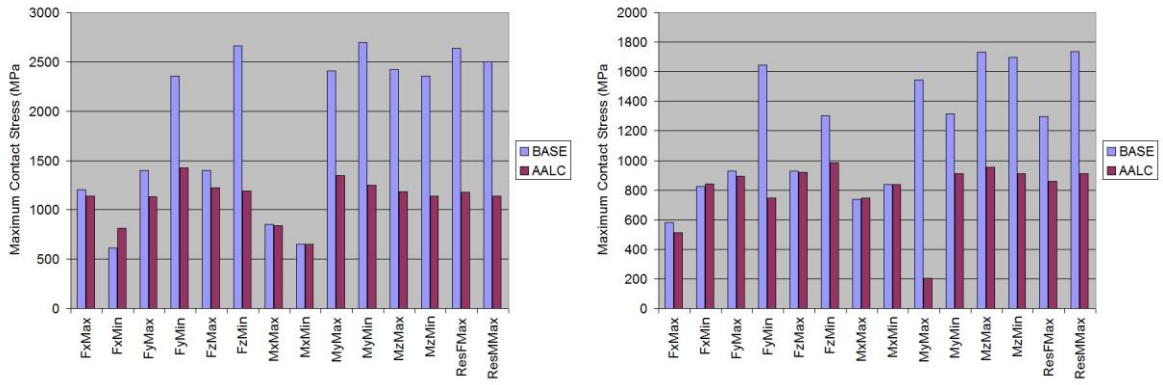

a) Upwind *b) Downwind*

Figure 8 Planetary carrier bearing contact stress results (BASE vs. AALC)

The investigation also has shown improvements in fatigue life of bearings. For these calculations, a fatigue load spectra in multiple dimensions is determined and for each load case in the spectra, the non-linear static analysis is performed with the RomaxWind model. The analysis results provide bearing loads and loaded contact distributions as well as other factors. These results are used to perform the fatigue calculations according to ISO 281[32] (and DIN ISO 281 Supplement 4). Table 1 provides a brief summary of the results for the bearings; it shows reductions in the fatigue damage as a result of the implementation of AALC; in particular, the upwind carrier bearing shows a reduction of 32%. Additional details and results are presented in the Romax project report[33].

Table 1 Impact of AALC on fatigue damage of bearings.

Bearing	Relative Change in Fatigue Damage due to AALC
Main	-7%
Upwind Carrier	-32%
Downwind Carrier	-16%

Active aero load control provides a remarkable improvement to the limiting stresses and fatigue for these load carrying bearings. This improvement would allow for a smaller, lower cost bearing and support structure in a new design or improved reliability and life when implemented to an existing design.

K. Impact of AALC on the Bedplate

Part of this research is to quantify the benefits of AALC to the supporting structures such as rotor hub, housings and bedplate. Here the bedplate stresses are studied for the peak load cases with maximum moments M_x, M_y and M_z (also with the loads in other directions that occur at the same time instant). A set of results is shown in Figure 9 - Figure 11; the loads are applied at the hub in the RomaxWind model and are reacted onto the bedplate through the main bearing and gearbox mounts (elements apart from the hub are hidden). The bedplate is constrained at the base. For the maximum M_x, which is torque, there is little benefit gained; AALC is not reducing the maximum torque experienced by the drivetrain. For the maximum off-axis moments (M_y and M_z) the benefits are again dramatic with significant reductions in the stresses at critical regions of the structure.

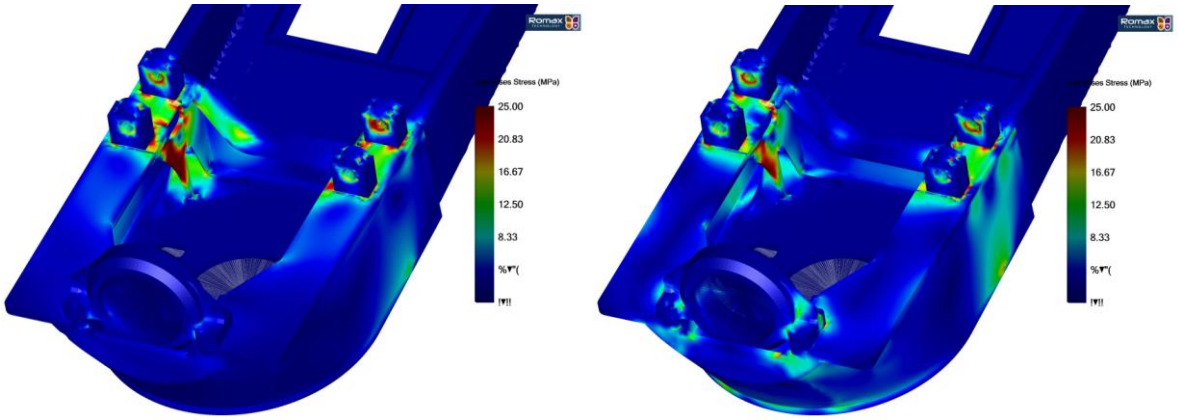

Figure 9 Bedplate stress results for max moment about the x-axis (rotor torque axis): BASE vs. AALC

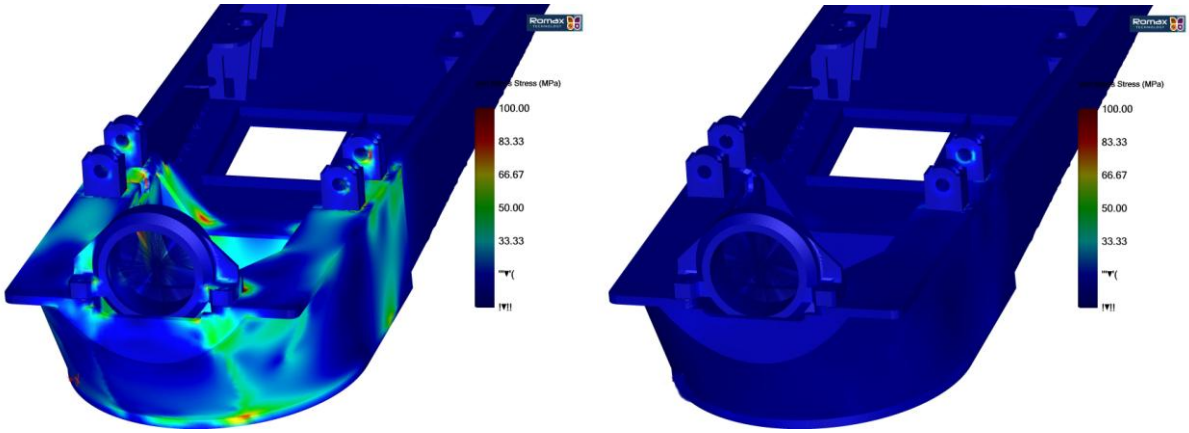

Figure 10 Bedplate stress results for max moment about the x-axis (non-torque axis): BASE vs. AALC

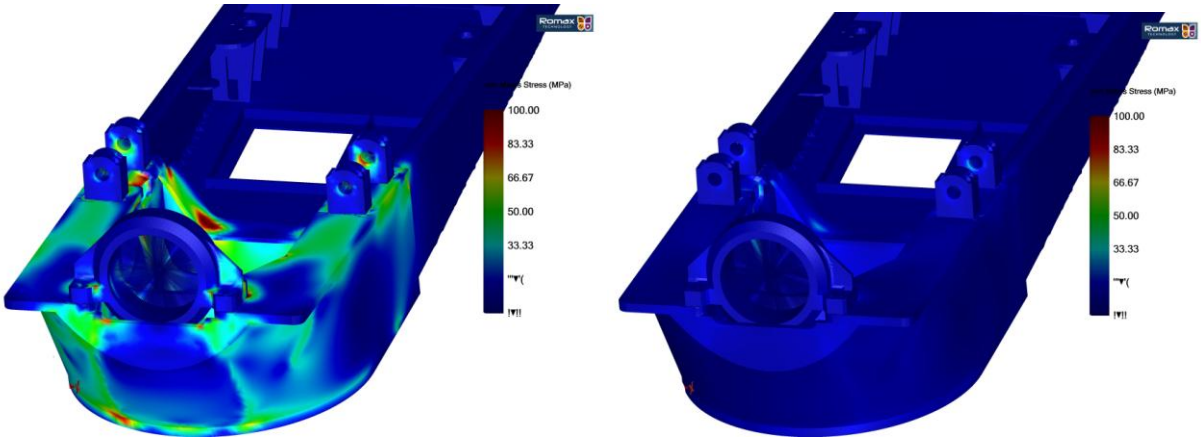

Figure 11 Bedplate stress results for max moment about the x-axis (non-torque axis): BASE vs. AALC

IV. Summary

This research reports a portion of the results on a project undertaken to determine the impact of AALC on various components in the wind turbine structural load path. The research demonstrates that AALC significantly reduces the peak loads that would be applied to the design calculations to confirm satisfactory component stresses versus limit criteria. A detailed computational model of the turbine drivetrain, including contact mechanics for the machine elements and elastic structures for bedplate, gearbox housings and shaft, was applied to quantifying such stresses. Peak load analyses demonstrated significant improvements in damage metrics when AALC was implemented. In particular, bearing contact stresses were reduced by as much as 50%. Fatigue analysis showed improvements between 7 and 32% for the load carrying bearings. Finally, this investigation shows reduction in bedplate stresses under peak loads when active aero is implemented.

V. Acknowledgment

The authors thank and recognize NREL staff who contributed to the creation of the FAST and AeroDyn model inputs to describe the GRC turbine. Availability of this model information was a critical enabler in this investigation.

VI. References

1. Global Wind Energy Council, 'Global Wind Power Boom Despite Economic Woes' *Press Release 3/2/2010*
2. Tavner, P.J., Spinato, F., van Bussel, G.J.W. and Koutoulakos, E, 'Reliability of Different Wind Turbine Concepts with Relevance to Offshore Application', *European Wind Energy Conferenc*e, Brussels, Belgium, 31 March – 3 April, 2008.
3. *Ladwirtschaftskammer (LWK)*, Schleswig-Holstein, Germany
4. Oyague, F., Butterfield, C.P. and Shuangwen, S., 'Gearbox Reliability Collaboration Analysis Round Robin', *NREL/CP-500-45325, May 2009*
5. http://windpower.sandia.gov/topical.htm#WPR, CREW Database and Analysis Program, Update, Sandia Blade Workshop, July 2010 - B.L. McKenney, A.B. Ogilvie (SAND Number: 2011-3437C)
6. U.S. Department of Energy, '20% Wind Energy by 2030: Increasing Wind Energy's Contribution to U.S. Electricity Supply', *DOE/GO-102008-2567*, July 2008.
7. Barlas, T.K. and van Kuik, G.A.M., 'Review of state of the art in smart rotor control research for wind turbines', *Progress in Aerospace Science (2009)*, doi:10.1016/j.paerosci.2009.08.002
8. van Wingerden, J-W., Hulskapp, A.W., Barlas, T., Marrant, B., van Kuik, G.A.M. and Molenaar, D-P, Verhaegen, M., 'On the Proof of Concept of a 'Smart' Wind Turbine Rotor Blade for Load Alleviation', *Wind Energy*, 2008; 11:265-80.
9. Barlas, T., van Wingerden, J-W., Hulskamp, A. and van Kuik, G., 'Closed-loop Control Wind Tunnel Tests on an Adaptive Wind Turbine Blade for Load Reduction', *Proceedings of the 46th AIAA/ASME*, Reno, NV, USA, 2008.
10. Troldborg, N. 'Computational Study of the Risø B1-18 Airfoil with a Hinged Flap providing Variable Trailing Edge Geometry', *Wind Engineering* 2005, 29:89-113.
11. Buhl, T., Gaunaa, M., and Bak, C., 'Load Reduction Potential using Airfoils with Variable Trailing Edge Geometry', *Proceedings of the 43th AIAA/ASME*, Reno, NV, USA, 2005.
12. Buhl, T., Gaunaa, M., and Bak, C., 'Potential Load Reduction using Airfoils with Variable Trailing Edge Geometry', *Solar Energy Engineering* 2005, 127:503-16.
13. Andersen, P. B., Gaunaa, M., Bak, C., and Buhl, T. 'Load Alleviation on Wind Turbine Blades using Variable Airfoil Geometry', *Proceedings of the EWEC* 2006, Athens, Greece.
14. Andersen, P. B., Gaunaa, M., Bak, C., and Buhl, T., 'Wind Tunnel Test on Wind Turbine Airfoil with Adaptive Trailing Edge Geometry', *Proceedings of the 45th AIAA/ASME*, Reno, NV, USA, 2007.
15. Buhl, T., 'Stability Limits for a Full Wind Turbine Equipped with Trailing Edge Systems', *European*

Wind Energy Conference, Marseille, France, 16-19 March, 2009.
16. Anderson, P.B., 'Load Reduction Using Pressure Difference on Airfoil for Control of Trailing Edge Flaps', *European Wind Energy Conference*, Marseille, France, 16-19 March, 2009.
17. Wilson, D.G., Berg, D.E., Barone, M.F., Berg, J.C., Resor, B.R., and Lobitz, D.W., 'Active Aerodynamic Blade Control Design for Load Reduction on Large Wind Turbines', *European Wind Energy Conference*, Marseille, France, 26-19 March, 2009.
18. Berg, D.E., Wilson, D.G., Barone, M.F., Berg, J.C., Resor, B.R., Paquette, J.A., and Zayas, J.R., 'The Impact of Active Aerodynamic Load Control on Fatigue and Energy Capture at Low Wind Speed Sites', *European Wind Energy Conference*, Marseille, France, 16-19 March, 2009.
19. Berg, D.E., Wilson, D.G., Resor, B.R., Barone, M.F., Berg, J.C., Kota, S. and Ervin, G., 'Active Aerodynamic Blade Load Control Impacts on Utility-Scale Wind Turbines', *WINDPOWER 2009*, Chicago, Illinois, 5-7 May, 2009.
20. Wilson, D.G., Berg, D.E., Resor, B.R., Barone, M.F., and Berg, J.C., 'Combined Individual Pitch Control and Active Aerodynamic Load Controller Investigation for the 5MW UpWind Turbine', *WINDPOWER 2009*, Chicago, Illinois, 5-7 May, 2009.
21. Berg, D.E., Wilson, D.G., Resor, B.R., Berg, J.C., Barlas, T., Crowther, A.R., and Halse, C., 'System ID Modern Control Algorithms for Active Aerodynamic Load Control and Impact on Gearbox Loading', *The Science of Making Torque from Wind*, Herkalion, Crete, Greece, 28-30 June, 2010.
22. Wright, Z., Halse, C., and Crowther, A.R., 'NREL Gearbox Engineering Assessment', Romax Technology Engineering Report for the National Renewable Energy Laboratory, March, 2011.
23. Crowther, A.R., Lockton, A., and Wright, Z., *'Technology Trends and Design Approaches for Wind Turbine Drivetrains', Proc. 8th IFToMM International Conference on Rotordynamics*, Sept 2010, Seoul
24. Bir, G.S., and Oyague, F., 'Estimation of Blade and Tower Properties for the Gearbox Research Collaborative Wind Turbine", *NREL/TP-500-42250*, November, 2007
25. Drela, M. and Giles, M.B., 'Viscous-Inviscid Analysis of Transonic and Low Reynolds Number Airfoils', *AIAA J*, 25(10):1347-1355, 1987.
26. NWTC Design Codes (AirfoilPrep by Craig Hansen). http://wind.nrel.gov/designcodes/preprocessors/airfoilprep/. Last modified 16-January-2007; accessed 16-January-2007.
27. NWTC Design Codes (FAST by Jason Jonkman), http://wind.nrel.gov/designcodes/simulators/fast/. Last modified 12-August-2005; accessed 12-August-2005.
28. NWTC Design Codes (Aerodyn by Dr. David Laino), http://wind.nrel.gov/designcodes/simulators/aerodyn/. Last modified 05-July-2005; accessed 05-July-2005.
29. MatLab/Simulink – *Matlab* version 7.3 release 2006b and *Simulink* version 6.5 release 2006b. The Mathworks Inc.
30. IEC TC88-MT1 (ed.). 'IEC 61400-1 Ed.3: Wind Turbines – Part 1: Design Requirements', International Electrotechnical Commission, Geneva, 2005.
31. NWTC Design Codes (TurbSim by Neil Kelley and Bonnie Jonkman), http://wind.nrel.gov/designcodes/preprocessors/turbsim/. Last modified 11-September-2008; accessed 11-September-2008.
32. ISO, 'Rolling Bearings – Dynamic Load Ratings and Rating Life', *International Standard ISO 281 2nd Edition 2007-02-15*.
33. Wright, Z., Crowther, A., and Halse, C., 'Assessment of the Impact of AALC on the Strength and Fatigue of the GRC Drivetrain', Romax Technology Engineering Report for Sandia National Laboratories, In Press (2011).